



**HAL**  
open science

# Effect of upstream and downstream pressure losses on flow reversals in low-pressure natural circulation loops

S. Renaudière de Vaux, B Grosjean

► **To cite this version:**

S. Renaudière de Vaux, B Grosjean. Effect of upstream and downstream pressure losses on flow reversals in low-pressure natural circulation loops. *Advances in Thermal Hydraulics 2022, ANS, Jun 2022, Anaheim, United States.* <cea-03968134>

**HAL Id: cea-03968134**

**<https://cea.hal.science/cea-03968134v1>**

Submitted on 1 Feb 2023

**HAL** is a multi-disciplinary open access archive for the deposit and dissemination of scientific research documents, whether they are published or not. The documents may come from teaching and research institutions in France or abroad, or from public or private research centers.

L'archive ouverte pluridisciplinaire **HAL**, est destinée au dépôt et à la diffusion de documents scientifiques de niveau recherche, publiés ou non, émanant des établissements d'enseignement et de recherche français ou étrangers, des laboratoires publics ou privés.



HAL Authorization

# Effect of Upstream and Downstream Pressure Losses on Flow Reversals in Low-Pressure Natural Circulation Loops

S. Renaudière de Vaux and B. Grosjean

CEA Cadarache (French Atomic Energy Commission), DES/IRENE/DER, Service d'Études des Systèmes Innovants (SESI),  
13108 Saint-Paul-lez-Durance, France  
sebastien.renaudierevaux@cea.fr; baptiste.grosjean@cea.fr

## INTRODUCTION

In the past years, strong interests have risen in the design of passive heat exchanger for the nuclear industry. In particular, Safety Condensers (SACOs) are designed to operate at pressures close to the atmospheric pressure. These designs combine several advantages, namely their inherent safety and robustness. Nevertheless, their stability regarding thermal hydraulics phenomena is strongly dependent on the design (geometry, pressure losses), but also on the expected working conditions (inlet temperature and wall heat flux). For instance, flowrate instability and reversal may induce vibrations or have thermomechanical effects on the exchanger.

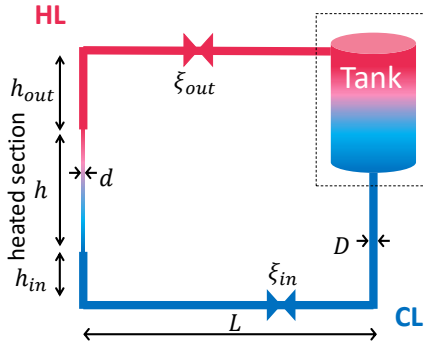


Fig. 1. Standard natural circulation loop investigated here.

We focused here on a standard two-phase natural circulation loop, as depicted in Fig. 1. The test section is constituted of a single cylindrical channel. The water, initially at temperature  $T_{in}$ , receives thermal power  $P_{in}$  through the heated section, rises and by mass conservation, it induces circulation through the whole loop. For low  $P_{in}$ , the water will not reach its boiling point, and the flow will remain liquid. Such loops are unconditionally stable [1]. On the opposite if  $P_{in}$  is large enough, boiling occurs in the heated section and nonlinear phenomena happen. Past works [2–12] have shown that natural circulation exchanger are stable at low  $P_{in}$  and high subcooling  $T_{sat} - T_{in}$  (with  $T_{sat}$  the saturation temperature), and exhibit strong flow reversals at high  $P_{in}$  and low  $T_{sat} - T_{in}$ . These works included theoretical, experimental and numerical studies. Stability analyses suggest that the destabilization results from density waves in the heated section [3]. Although the findings are consistent on the boundary shape between these two regimes, it is strongly dependent on upstream and downstream hydraulic conditions, i.e. on the exchanger and loop designs. In this summary, we investigate numerically and experimentally the influence of upstream and downstream pressure losses on the

stability boundaries. A dedicated platform called EXOCET<sup>1</sup> has been built in CEA Cadarache (France) to study their influence and a 1D numerical model of the facility was developed with the thermal-hydraulic code CATHARE [13]. We compare and validate our data with results from [12], as the geometrical data is close to ours, and investigate the effects of pressure losses on the stability diagram with experimental results from the EXOCET facility.

We first describe the physical problem and define quantities of interest, which are the phase change number  $N_{pch}$  and the subcooling number  $N_{sub}$  (later defined). In the results section, we describe and discuss our results, regarding comparison of experimental and numerical data. Once the validation is carried out, we discuss the influence of the input parameters and of the upstream and downstream pressure losses on the flowrate.

## PROBLEM MODELING

### Physical Modeling

We perform a dimensional analysis to establish relevant nondimensional parameters for the study. Given a standard circulation loop as shown in Fig. 1, we assume that in the tank there is a perfect heat exchanger and at the tank exit, the temperature is constant  $T_{in}$  and the absolute operating pressure  $P$  is fixed. We also assume that the cold leg (CL) and hot leg (HL) are constituted of adiabatic walls. We follow [4, 6] in establishing nondimensional quantities. First we determine reference values for velocity, time, mass flowrate and input power. Su et al. [14] determined the reference velocity for a closed-square natural circulation channel as

$$U_{ref} = \left( \frac{gdRe_{ref}^{0.241}}{0.416} \right)^{1/2}, \quad (1)$$

with  $Re_{ref} = U_{ref}d/\nu_l$  the characteristic Reynolds number of the loop. Solving for the reference velocity gives

$$U_{ref} = \frac{1.62g^{0.569}d^{0.705}}{\nu_l^{0.137}}. \quad (2)$$

Here all dimensions and physical quantities are taken in SI units. The characteristic velocity  $U_{ref}$  takes into account the acceleration of gravity  $g$ , the heated section diameter  $d$  and the kinematic liquid viscosity  $\nu_l$ . As suggested in [5–7], we

<sup>1</sup>for EXpérience d'Observation du Chouage d'Échangeur Tertiaire

TABLE I. Values of  $N_{pch}$  and  $N_{sub}$  for the considered configurations.

	[12]	[12]	EXOCET	EXOCET
$P$ [bar]	3	4	1.1	1.7
$N_{sub}$ [-]	40-80	30-65	50-250	50-180
$N_{pch}$ [-]	7-20	5-20	0-25	0-20

then define the reference quantities as

$$t_{ref} = h/U_{ref}; \quad (3a)$$

$$Q_{ref} = \rho_l U_{ref} S; \quad (3b)$$

$$P_{ref} = Q_{ref} L_{lv} \frac{\rho_v}{\rho_l - \rho_v}. \quad (3c)$$

Here the reference time  $t_{ref}$  is the characteristic time of rising through the heated section of height  $h$  at the velocity  $U_{ref}$ . The characteristic mass flowrate is the flowrate through the heated section of cross-section  $S = (\pi d^2)/4$ . The characteristic input power  $P_{ref}$  is a function of  $Q_{ref}$ , the latent heat  $L_{lv}$  and the liquid and vapor densities  $\rho_l$  and  $\rho_v$ . All physical quantities are computed at the saturation temperature  $T_{sat}$  for each operating pressure. According to [4, 6], we define the phase change and the subcooling numbers as

$$N_{pch} = \frac{P_{in}}{P_{ref}}; \quad (4a)$$

$$N_{sub} = \frac{c_{p,l}(T_{sat} - T_{in})(\rho_l - \rho_v)}{L_{lv}\rho_v}, \quad (4b)$$

with  $P_{in}$  the input power,  $c_{p,l}$  the liquid heat capacity,  $T_{sat}$  the saturation temperature,  $T_{in}$  the inlet temperature. According to [4], these two parameters are the main ones governing stability. The other nondimensional groups are either outputs of the system or quasi-constant. The range of  $N_{pch}$  and  $N_{sub}$  is given in Table I for each configuration.

With these definitions, a steady-state enthalpy balance over the heated test section gives

$$N_{pch} = Q_{av}^* \left( N_{sub} + x_v \frac{\rho_l - \rho_v}{\rho_v} \right), \quad (5)$$

with  $x_v$  the vapor quality and  $Q_{av}^*$  the average nondimensional mass flowrate. Here we see that  $Q_{av}^*$  and  $x_v$  are related by Eq. (5) and by the nonlinear momentum balance and mass conservation. These equations are solved using the CATHARE code.

### Numerical Modeling with CATHARE

We use the system-scale code CATHARE to solve thermal-hydraulics in the natural circulation loop. The code is a two-fluid six-equation model based on finite differences for scalar fields and finite volumes for vector fields [13]. Moreover, heat conduction in the wall is computed, between the internal and external sides, using three cells. The CATHARE simulation is initialized with homogeneous pressure and zero velocity. First no power is provided and the code converges to the hydrostatic state. Then the input power is progressively

imposed by a linear ramp during 500 s. After the transient regime, a steady-state regime is reached. We focused here on the steady-state regime. The robustness of the model with regard to the mesh was checked in a separate study. As shown in Fig. 2, three types of regimes were identified, based on the time-evolution of the nondimensional flowrate  $Q^*(t^*)$ , similarly to the experimental results from [12]:

1. Stable regime : constant flowrate  $0.1 \leq Q^*(t^*) = Q_{av}^* \leq 0.4$ ;
2. Oscillatory regime : oscillating flowrate which remains positive  $Q^*(t^*) \geq 0$ , and with average  $0.3 \leq Q_{av}^* \leq 0.6$ ;
3. Flow reversal regime : strongly oscillating flowrate which becomes negative. In extreme cases, the maximum acceptable pressure or temperature were reached, which lead to stopping the computation.

In general, when the computation stopped, it occurred after several cycles of flow reversals. Therefore, this regime is well observed and it highlighted the possibility of strong temperature or pressure increase. The observed regimes are discussed in the following Section.

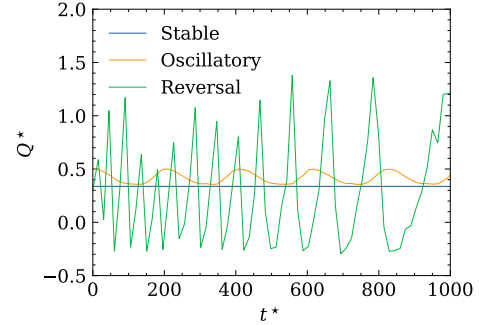


Fig. 2. Types of regimes observed based on the time evolution of  $Q^*$ .

## RESULTS AND ANALYSIS

### Comparison with Results from Chen et al. [12]

Based on geometrical data from [12] and pressure losses estimates from [15], upstream and downstream equivalent singular pressure loss coefficients  $\xi_{in}$  and  $\xi_{out}$  were estimated between 1 and 100. A sensitivity study with  $\xi_{out} = 1$  and 100 was carried out and has not highlighted significant differences in the stability diagram. Computations were carried out on a large number of  $(N_{pch}, N_{sub})$  for a geometry close to [12]. An example of stability diagram is shown in Fig. 3. There is a great agreement on the stability domains obtained in [12] and obtained with CATHARE. In both cases, the boundary is given by a straight line of similar slope and origin. For the experimental case, a thin zone of oscillatory flows between the two domains is observed. This situation was difficult to reproduce numerically as the step for the computation grid was larger than the zone width. Moreover, experimental boundary between the stable regime and the unstable ones is given by

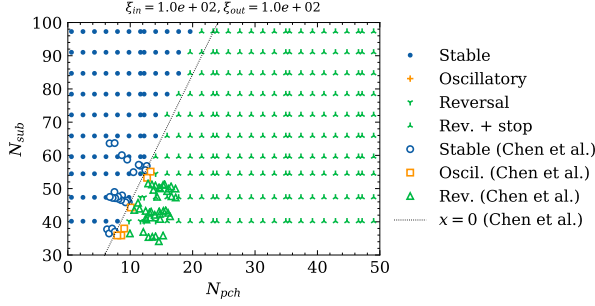


Fig. 3. Phase diagram obtained with CATHARE at  $P = 3$  bar compared with [12].

$x_v = 0$ , meaning that instabilities are linked to significant vapor apparition. Moreover, in [12], the condensation tank was placed horizontally, contrary to the numerical model used here.

### Comparison with EXOCET Results

For the EXOCET facility, it was assumed that  $1 \leq \xi_{in}, \xi_{out} \leq 10^6$ , and depends on the valve opening  $x_{in}$  or  $x_{out}$  only. An example of singular pressure loss coefficient  $\xi_{out}$  as a function of the valve opening  $x_{out}$  is given in Fig. 4. To estimate them, flowrate (i.e. the Reynolds number  $Re = UD/\nu_l$ ) was fixed in the loop and no heating was provided; and  $\xi_{out} = \Delta P_{out} / \frac{1}{2} \rho_l U^2$  was monitored, with  $\Delta P_{out}$  the pressure difference upstream and downstream of the valve. It is seen that  $\xi_{out}$  mainly depends on the valve opening. We observe that the dependence of  $\xi_{out}$  with  $x_{out}$  is strong for  $x_{out} \leq 40\%$ . On the contrary, the curve is nearly flat for  $x_{out} \geq 60\%$ , and in this region  $\xi_{out}$  weakly depends on  $x_{out}$ . Nevertheless, there is a strong dispersion of experimental data. For example with a given  $x_{out}$ , the experimental value of  $\xi_{out}$  may vary by a factor 2 for  $x_{out} \geq 40$ . The dispersion is higher for lower  $x_{out}$ . Therefore, this may lead to additional uncertainty in determining experimental and numerical regime boundaries. Another source of uncertainty lies in the fact that  $\xi_{out}$  was determined with an imposed isothermal flow, whereas in an actual case the flow is not imposed, and two-phase phenomena may also influence its value.

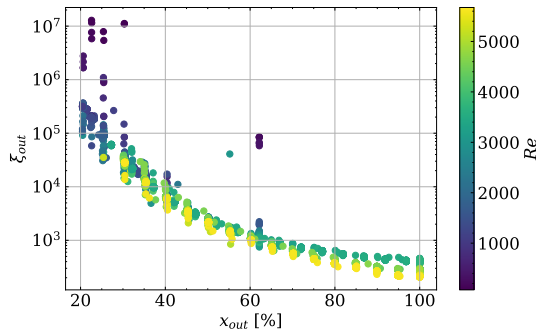


Fig. 4. Singular downstream pressure loss coefficient  $\xi_{out}$  as a function of the valve opening  $x_{out}$ , with an imposed isothermal flow.

In the EXOCET experiments,  $P_{in}$  was progressively im-

posed, initially with fully opened valves. It was observed that the upstream valve had no influence on the stability boundaries, both experimentally and numerically. The downstream valve was then progressively closed (i.e.  $\xi_{out}$  was increased) until the apparition of flow reversals. The stability boundaries were then reconstructed in the  $(N_{pch}, N_{sub})$ -plane by interpolating the boundaries. The results are shown in Fig. 5, with experimental data as dots. The stability boundaries for different values of valve opening  $x_{out}$  are straight lines, similarly to the observations of [12]. For a given  $x_{out}$ , the region above the boundary is stable and the region below it is unstable.

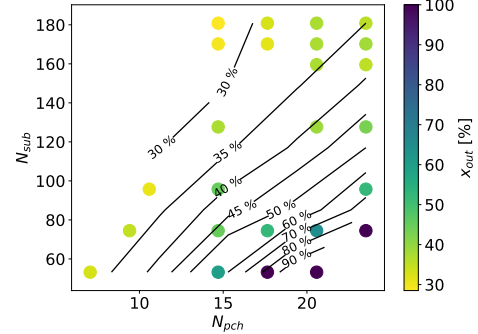


Fig. 5. Experimental phase diagram of EXOCET. The dots show the experimental data points and the colors show the valve opening  $x_{out}$  at which reversal was observed. The lines are the interpolated boundaries for various  $x_{out}$ .

Based on Fig. 4, we see that a valve opening  $x_{out} \approx 40\%$  corresponds to  $\xi_{out} \approx 10^4$ . The comparison of EXOCET experimental results with the numerical results is given in Fig. 6. There is a good agreement between experimental and numerical data. However, uncertainties on the estimate of  $\xi_{out}$  lead to slight difficulties in reproducing exactly the same boundaries.

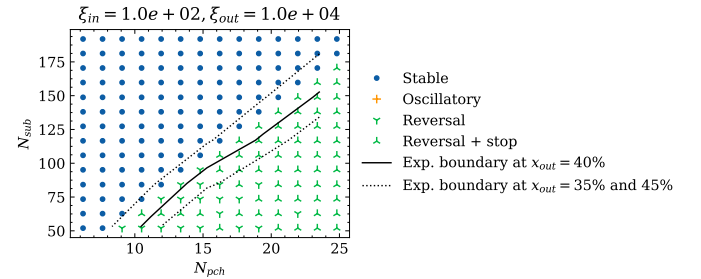


Fig. 6. Example of phase diagram obtained with CATHARE in the EXOCET configuration and comparison with experimental results at  $P = 1.1$  bar. Here, the valve opening  $x_{out} \approx 40\%$  corresponds to  $\xi_{out} \approx 10^4$ . The dotted lines show the experimental stability boundaries for  $\pm 5$  percentage points of valve closing/opening.

Indeed as seen in Fig. 4 for fully open valves, there is an uncertainty on the  $\xi_{out}$  value, as it is comprised between 100 and  $10^3$ . A sensibility study with CATHARE for  $1 \leq \xi_{in} = \xi_{out} \leq 10^3$  was carried out in the stable regime and the results are shown by the lines in Fig. 7 for three values of  $N_{pch}$ .

In general  $Q_{av}^*$  decreases with  $N_{sub}$ . It is observed that the singularities have a weak influence on  $Q_{av}^*$  in the stable regime. Moreover, experimental results are shown by the symbols, with fully open valves. In the stable regime for  $N_{sub} \geq 100$ , there is an excellent agreement between experimental and numerical data. For lower values of  $N_{sub}$ , the agreement is less good. The flow is closer to the instability boundary, and the destabilization mechanism becomes highly sensitive to the input parameters. Nevertheless, as highlighted before, there is an excellent agreement between the phase diagrams.

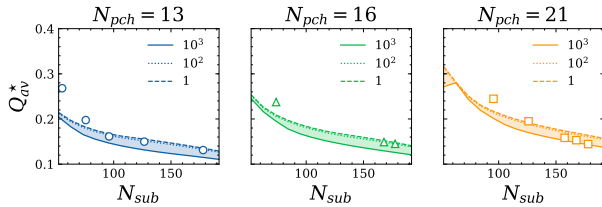


Fig. 7. Flowrate sensitivity analysis. The shaded area shows the possible flowrates for  $1 \leq \xi_{in}, \xi_{out} \leq 10^3$ . In all cases shown here, we fixed  $\xi_{in} = \xi_{out}$ .

## CONCLUSIONS

In this summary, we have highlighted new numerical and experimental results that show the capacity of the CATHARE code to predict quantitatively flow reversals in natural circulation loops. The numerical results were compared to available results from the literature [12] and with recent results obtained from the EXOCET facility in CEA Cadarache, and showed excellent agreement. For low  $N_{pch}$  and high  $N_{sub}$ , the flow is stable and for high  $N_{pch}$  and low  $N_{sub}$  the system exhibits flow reversals.

The boundary between these regimes is given by a straight line in the  $(N_{pch}, N_{sub})$ -plane, whose slope and origin depend essentially on the downstream pressure loss coefficient  $\xi_{out}$ , and practically not on the upstream coefficient  $\xi_{in}$ . Between the two regions, a thin zone with flow oscillation and without reversals exists, but is difficult to observe numerically.

We showed that increasing  $\xi_{out}$  favors flow reversals and drastically reduces the stable area. In the context of nuclear safety, it is essential to design heat exchangers for which the flow will remain stable, and therefore reduce the downstream pressure losses. In the future, it could be interesting to study the time frequency of flow reversals, or to focus on the geometry of the heated section.

## ACKNOWLEDGMENTS

The design of the EXOCET facility and the experiments were carried out by Lionel Rossi, Philippe Aubert and Sylvain Vitry from DTN in CEA Cadarache. The authors kindly thank them for sharing their results and for fruitful discussions. This work has been funded by the Nuward™ industrial project which is currently developing a PW-SMR nuclear power plant.

## REFERENCES

1. P. K. VIJAYAN, A. K. NAYAK, and N. KUMAR, *Single-phase, Two-phase and Supercritical Natural Circulation Systems*, Woodhead Publishing (2019).
2. M. ISHII, *Thermally induced flow instabilities in two-phase mixtures in thermal equilibrium*, Georgia Institute of Technology (1971).
3. M. ISHII, "Study on flow instabilities in two-phase mixtures," Tech. rep., Argonne National Lab., IL (USA) (1976).
4. M. ISHII and I. KATAOKA, "Scaling criteria for LWR's under single-phase and two-phase natural circulation," Tech. rep., Argonne National Lab., IL (USA) (1982).
5. Y. LIN and C. PAN, "Non-linear analysis for a natural circulation boiling channel," *Nuclear Engineering and Design*, **152**, 1-3, 349–360 (1994).
6. S. WANG, J. WU, P. CHIN, and W. LIN, "Thermal-hydraulic oscillations in a low pressure two-phase natural circulation loop at low powers and high inlet subcoolings," in "4th International Topical Meeting on Nuclear Thermal Hydraulics, Operations and Safety," (1994).
7. C. WU, S. WANG, and C. PAN, "Chaotic oscillations in a low pressure two phase natural circulation loop under low power and high inlet subcooling conditions," *Nuclear engineering and design*, **162**, 2-3, 223–232 (1996).
8. Z. GUOZHI, C. XINRONG, and S. XINGWEI, "A study using RELAP5 on capability and instability of two-phase natural circulation flow under passive external reactor vessel cooling," *Annals of Nuclear Energy*, **60**, 115–126 (2013).
9. S. SHI, J. P. SCHLEGEL, C. S. BROOKS, Y.-C. LIN, J. EOH, Z. LIU, Q. ZHU, Y. LIU, T. HIBIKI, and M. ISHII, "Experimental investigation of natural circulation instability in a BWR-type small modular reactor," *Progress in nuclear energy*, **85**, 96–107 (2015).
10. S. SHI, T. HIBIKI, and M. ISHII, "Startup instability in natural circulation driven nuclear reactors," *Progress in Nuclear Energy*, **90**, 140–150 (2016).
11. M. ISHII, "Investigation of Natural Circulation Instability and Transients in Passively Safe Small Modular Reactors," Tech. rep., Purdue Univ., West Lafayette, IN (United States) (2016).
12. X. CHEN, P. GAO, S. TAN, Z. YU, and C. CHEN, "An experimental investigation of flow boiling instability in a natural circulation loop," *International Journal of Heat and Mass Transfer*, **117**, 1125–1134 (2018).
13. R. PRÉA, P. FILLION, L. MATTEO, G. MAUGER, and A. MEKKAS, "CATHARE-3 V2.1: The new industrial version of the CATHARE code," in "Advances in Thermal Hydraulics, Palaiseau," (2020).
14. Y. SU, C. CHANG, and C. LEE, "Experimental study of natural circulation in a rectangular closed loop," in "Proc. 2nd World Conf. on Experimental Heat Transfer, Fluid Mechanics and Thermodynamics, Dubrovnik," (1991).
15. I. IDEL'CIK and M. MEURY, *Memento des pertes de charge: coefficients de pertes de charge singulières et de pertes de charge par frottement*, Eyrolles Paris (1986).